Griffiths, D. V. & Yu, X. (2015). *Géotechnique* **65**, No. 10, 824–830 [http://dx.doi.org/10.1680/geot.14.T.030]

Another look at the stability of slopes with linearly increasing undrained strength

D. V. GRIFFITHS*† and X. YU*

The paper presents a new look at the stability of slopes with linearly increasing undrained strength with depth. Particular emphasis in the current work is focused on the influence of a firm stratum on the factor of safety and the location of the critical failure surface. Solutions have been obtained by the application of standard optimisation software with some independent finite-element checks. Results are presented in the form of improved charts that give the stability number, and hence the factor of safety, as a function of the depth ratio, strength gradient and slope angle. It is shown that when the strength at the crest is greater than zero, previously published results can greatly underestimate the factor of safety, as the depth to a firm stratum is reduced.

KEYWORDS: finite-element modelling; limit equilibrium methods; shear strength; slopes

INTRODUCTION AND BACKGROUND

The stability of undrained ($\phi_u = 0$) slopes with linearly increasing strength with depth has long been of interest to geotechnical investigators, with important early work reported by Gibson & Morgenstern (1962) and Hunter & Schuster (1968). The problem definition is given in Fig. 1, where the slope height is H, the slope angle is β and the depth ratio to a firm stratum is D.

The variation of the undrained strength is given by the equation

$$c_u(z) = c_{u0} + \rho z \tag{1}$$

where c_{u0} is the strength at crest level ($z = 0$) and ρ is the gradient of strength increase with depth z. The parameter H_0 is the height above the crest at which the extrapolated undrained shear strength would reduce to zero. The saturated unit weight γ is assumed to be constant.

Hunter & Schuster (1968) considered the case of $c_{u0} > 0$ and introduced a dimensionless strength gradient parameter M, defined as

$$M = \frac{H_0}{H} \tag{2}$$

which can also be written as

$$M = \frac{c_{u0}}{\rho H} \tag{3}$$

and provided charts (in their figure 6) giving a dimensionless stability number N as a function of β, D and M. The stability number N is proportional to the factor of safety, FS, as shown in equation (4).

$$FS = N\frac{\rho}{\gamma} \tag{4}$$

Hunter and Schuster's charts indicate that N is significantly affected by β and M, but only marginally affected by D. The influence of D on the location of the critical failure mechanism and stability number will be the main focus of this paper.

Other investigators of the linearly increasing strength stability problem with $c_{u0} > 0$ include Koppula (1984), who performed similar optimisation analyses to those of Hunter & Schuster (1968) with improvements pointed out by Shen & Brand (1985), and Yu *et al.* (1998) who used the problem as a benchmark for comparison of finite-element limit analysis and limit equilibrium solutions.

The special case of $c_{u0} = 0$ ($M = 0$) was considered in detail by Gibson & Morgenstern (1962), who showed that the stability number N depends only on β. It was further shown that for any value of β, there exists an infinite number of critical circles all giving the same N. In a later section, the geometric range of the infinite family of circles giving the same stability number will be discussed. The special case of $c_{u0} = 0$ was also investigated by Booker & Davis (1972) using plasticity theory.

OPTIMISATION

Interested readers are referred to the online supplementary data for detailed information on the derivation of equations and the Matlab optimisation programs used to generate the results presented in this paper. In brief, a potential circular failure mechanism was postulated tangent to a given depth ratio D. Based on the geometry and strength distribution, equations were set up to compute the overturning and restoring moments, M_O and M_R, respectively, leading to a factor of safety given by

$$FS = \frac{M_R}{M_O} \tag{5}$$

The optimisation software was then used to find the location of the circle centre giving the minimum factor of safety. Finally the stability number was computed from equation (4) as

$$N = FS\frac{\gamma}{\rho} \tag{6}$$

The results presented in this paper for $N = f(\beta, M, D)$ all derive from equation (6).

Manuscript received 20 October 2014; revised manuscript accepted 17 April 2015. Published online ahead of print 28 July 2015. Discussion on this paper closes on 1 March 2016, for further details see p. ii.

* Colorado School of Mines, Golden, Colorado, USA.
† Australian Research Council Centre of Excellence for Geotechnical Science and Engineering, University of Newcastle, Callaghan, NSW, Australia.

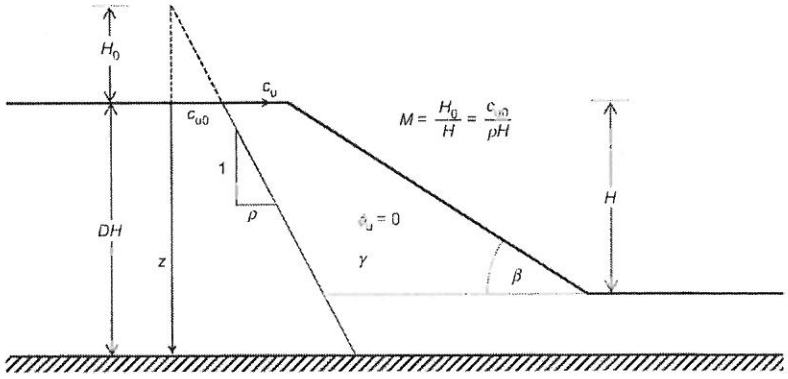

Fig. 1. Undrained slope with linearly increasing strength

INFLUENCE OF THE DEPTH RATIO

A full set of results for different parametric combinations with $c_{u0} > 0$ is given later in this section, but in order to explain the trends in more detail, a typical set of results for the case of a slope with $M = 2$ and $\beta = 15°$ is considered first, as shown in Fig. 2.

Four failure regions are identified for different ranges of D.

(*a*) Deep circle, $D \geq 2{\cdot}02$. A minimum stability number is observed at $D = 2{\cdot}02$, so the dashed curved line in the range $D > 2{\cdot}02$ given by the optimisation results is not critical, and the correct result just extends horizontally at $N = 22{\cdot}93$. In this range marked 'D', the critical failure surface outcrops to the right of the toe, but is not tangent to the strong layer below, which has no influence on the result, as shown in Fig. 3(a).

(*b*) Base circle, $2{\cdot}02 > D \geq 1{\cdot}54$. In this range marked 'B', the strong layer starts to influence the stability number N causing it to rise gradually as D is reduced. The critical failure surfaces are base circles and tangent to the strong layer below, as shown in Fig. 3(b).

(*c*) Toe circle, $1{\cdot}54 < D \leq 1{\cdot}37$. In this range marked 'T', the critical circles all pass through the toe and are tangent to the strong layer below, as shown in Fig. 3(c) and Fig. 4. The stability number N continues to rise as D is reduced.

(*d*) Slope circles, $D < 1{\cdot}37$. In this range marked 'S', the critical circles outcrop on the slope and are tangent to the strong layer, as shown in Fig. 3(d). The stability number N continues to rise more steeply as D is reduced.

As was noted by Shen & Brand (1985), the critical deep and base circles are always 'mid-point' circles; that is, the centre of the critical circle is exactly above the mid-point of the slope. As a further check, elastic–plastic finite-element results using a strength reduction algorithm are also shown

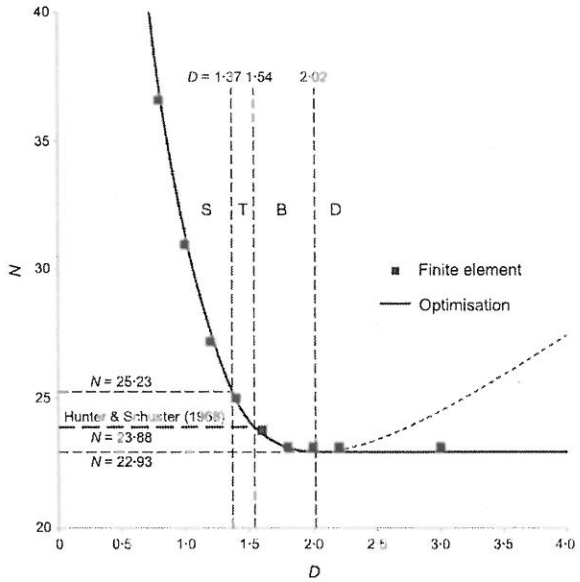

Fig. 2. Typical result for slope with $M = 2$ and $\beta = 15°$; S, slope; T, toe; B, base; D, deep

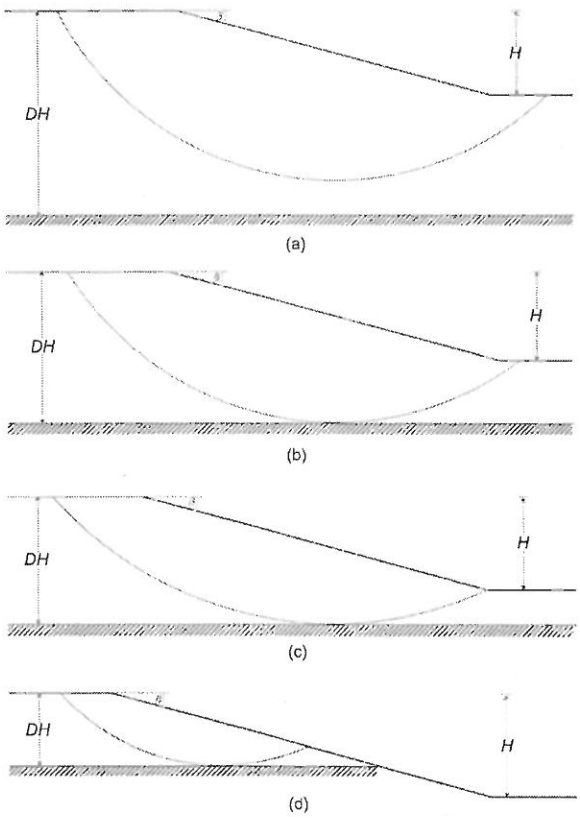

Fig. 3. Different types of critical failure circles: (a) deep circle (D) (D has no influence on N); (b) base circle (B); (c) toe circle (T); (d) slope circle (S)

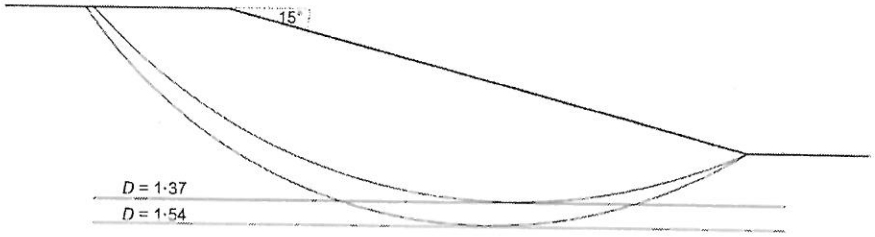

Fig. 4. Range of D values for which toe circles are critical when $M=2$ and $\beta=15°$

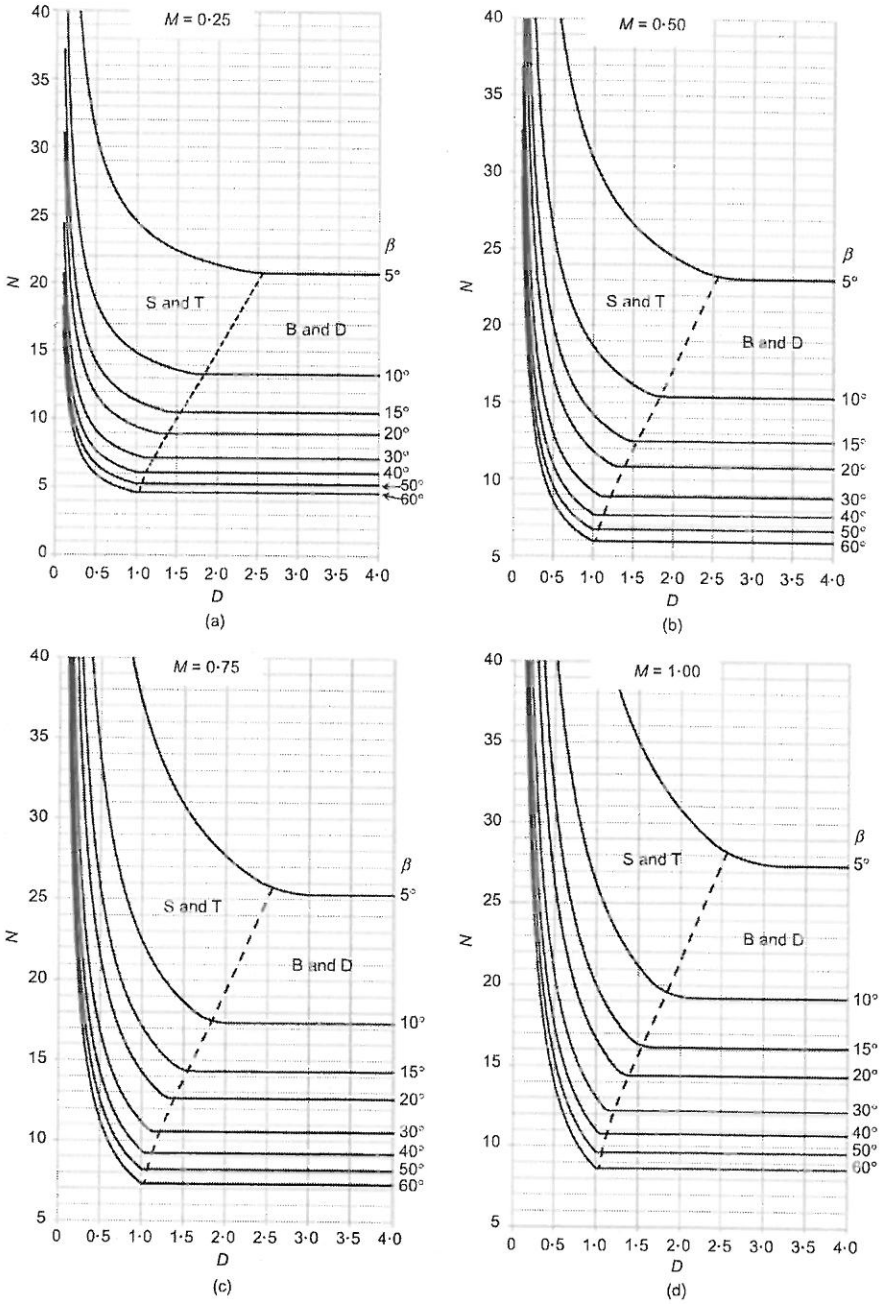

Fig. 5. Stability number (N) plotted against depth ratio (D): (a) $M=0·25$; (b) $M=0·50$; (c) $M=0·75$; (d) $M=1·00$; (e) $M=1·25$; (f) $M=1·50$; (g) $M=1·75$; (h) $M=2·00$ (continued on next page)

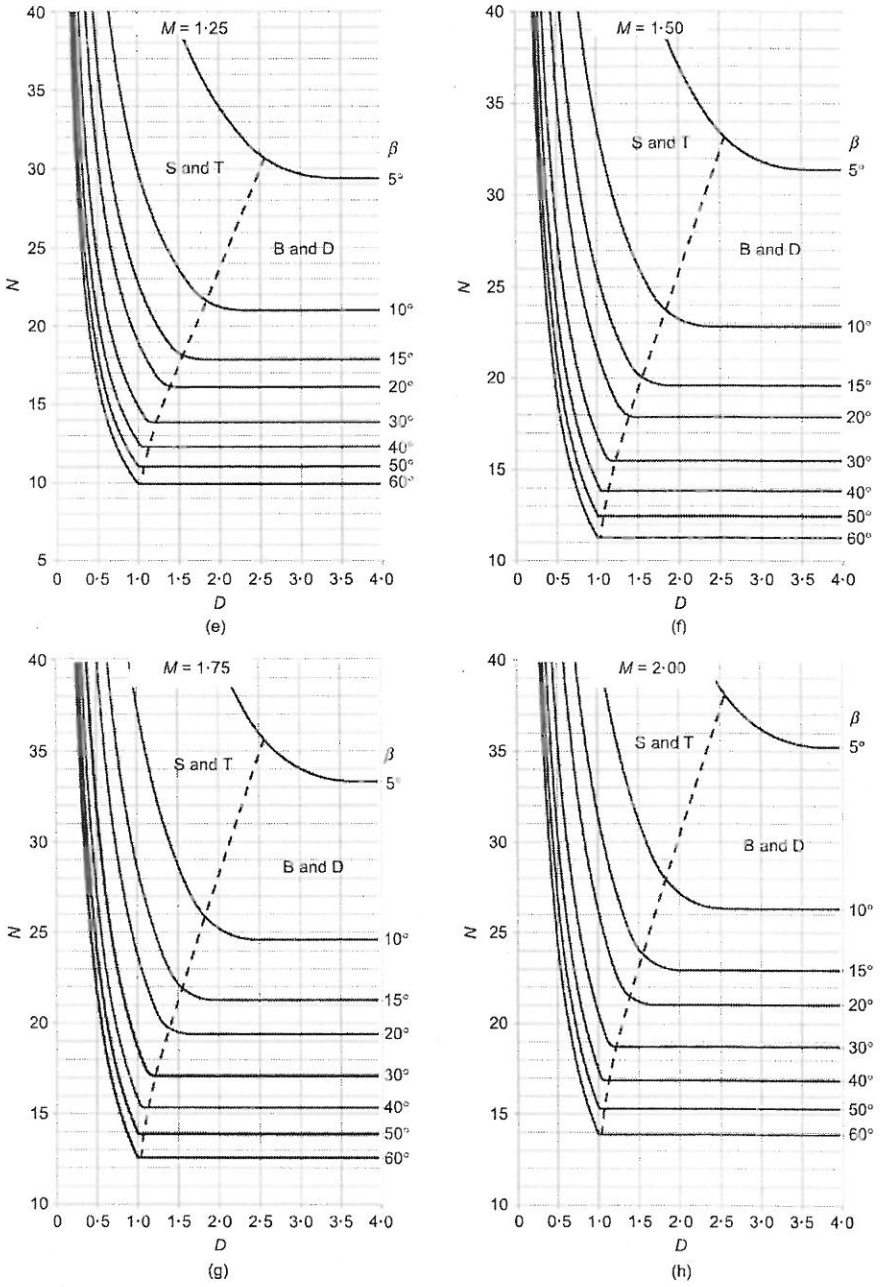

Fig. 5. Continued

in Fig. 2. The results confirm the trend given by the solid line, and the finite-element failure mechanisms also closely followed those indicated in Fig. 3 over the range of D values considered.

A more complete set of results for N plotted against D is now given in Fig. 5. For ease of comparison with figure 6 from Hunter & Schuster (1968), the same ranges of values they used, namely $0{\cdot}25 \leq M \leq 2$ and $0 < D \leq 4$ are presented. For each value of M, several slope angles are considered in the range $5° \leq \beta \leq 60°$. A dashed line is shown corresponding to the transition from deep and base circles, to toe and slope circles. Interested readers are also encouraged to use the Matlab programs provided in the supplementary data to investigate other cases.

Comparison with other investigators

The results presented in this paper agree exactly with Hunter & Schuster (1968) whenever the critical failure surface is of the deep or base type, as shown in Figs 3(a) and 3(b) and marked 'B and D' in Fig. 5; in other words, the results agree whenever the critical circle outcrops to the right of the toe. Results significantly disagree, however, whenever the critical failure surface is of the toe or slope type, as shown in Figs 3(c) and 3(d) and marked 'S and T' in Fig. 5. In this range the stability number N is shown to rise steeply as D is decreased, in contrast to Hunter and Schuster's results, which indicate a constant stability number (compare for example, the curved solid line and the horizontal dashed line marked 'Hunter & Schuster (1968)' in Fig. 2 when $D < 1{\cdot}54$).

Table 1. Geometry and properties for example problem

β	H	D	c_{u0}	ρ	γ	M (equation (3))
15°	10 m	1	20 kPa	1 kN/m^3	20 kN/m^3	2

A further observation on the comparison between results presented in this paper and those of Hunter and Schuster applies in cases where $D<1$. For example, a slope with height H, depth ratio $D=0{\cdot}5$ and strength gradient parameter M, is clearly identical to a slope with height $0{\cdot}5H$, depth ratio $D=1$ and strength gradient parameter $2M$ (assuming the same β, c_{u0}, ρ and γ). The charts presented in Fig. 5 of this paper reflect this exact equivalence, while the charts in figure 6 of Hunter & Schuster (1968) would give quite different stability numbers.

Example problem

The improved solutions presented in this paper are now illustrated with an example problem with geometry and properties shown in Table 1.

Figure 5(h) with $\beta=15°$ and $D=1$, gives a stability number of $N\approx 31{\cdot}42$, and a factor of safety from equation (4) of $FS=N(\rho/\gamma)=1{\cdot}57$. The Hunter & Schuster (1968) results from Fig. 2 with the same input parameters give $N\approx 23{\cdot}88$ and $FS=1{\cdot}19$; some 32% lower. This discrepancy could lead to very different slope design outcomes, since the lower and upper values of $FS=1{\cdot}19$ and $FS=1{\cdot}57$ might typically lie on either side of an acceptable target value of $FS=1{\cdot}5$. Lower values of $D<1$ would lead to ever greater differences between factors of safety predicted by the two methods.

Zero strength at the crest level, $c_{u0}=0$

The special case of linearly increasing undrained strength from zero strength at the crest level ($M=0$) was considered by Gibson & Morgenstern (1962). Those authors noted that the stability number, and hence the minimum factor of safety, depends only on the slope angle β, and is not influenced by the depth ratio D. Their results have been plotted as Fig. 6(a), and for consistency of presentation with Fig. 5, stability numbers for this case have also been plotted in Fig. 6(b), emphasising the insensitivity of N to the value of D.

Gibson and Morgenstern noted that for any given slope angle, there is an infinite family of critical circles, all giving the same stability number. The deepest circle in the infinite family of critical circles for a $\beta=15°$ slope is shown in Fig. 7(a), together with a couple of shallower ones. All circles indicated are critical, and give the same stability number of $N=8{\cdot}51$. The deepest circle passes through the toe with a positive gradient, and is tangent to a depth ratio of $D=1{\cdot}37$. Fig. 7(b) shows similar results for a $\beta=45°$ slope where all critical circles give $N=4{\cdot}11$. In this case, the deepest critical circle in the family is tangent to $D=1$ at the toe. For slopes steeper than 45°, the deepest circle in the family has a negative gradient as it passes through the toe as shown in Fig. 7(c) for a $\beta=75°$ slope. In this case all critical circles give $N=2{\cdot}56$.

A summary of the deepest depth ratio D of families of critical circles for different slope angles in the $M=0$ case is given in Fig. 8. It is clear from the figure that for flatter slopes where $\beta<45°$, the deepest critical circle can extend quite a way into the foundation soil if allowed. For example, from Fig. 8, for a $\beta=5°$ slope, the critical circle could be as deep as $D=2{\cdot}38$. This observation is at variance with

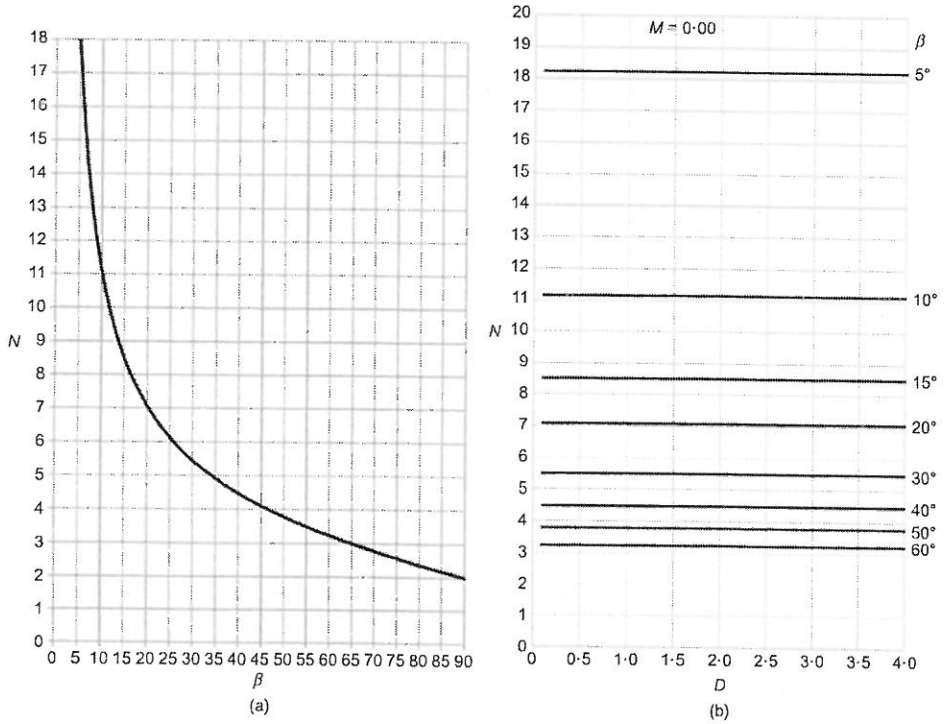

Fig. 6. Stability numbers for $M=0$ showing: (a) a unique relationship between β and N (after Gibson & Morgenstern, 1962); (b) insensitivity of N to D

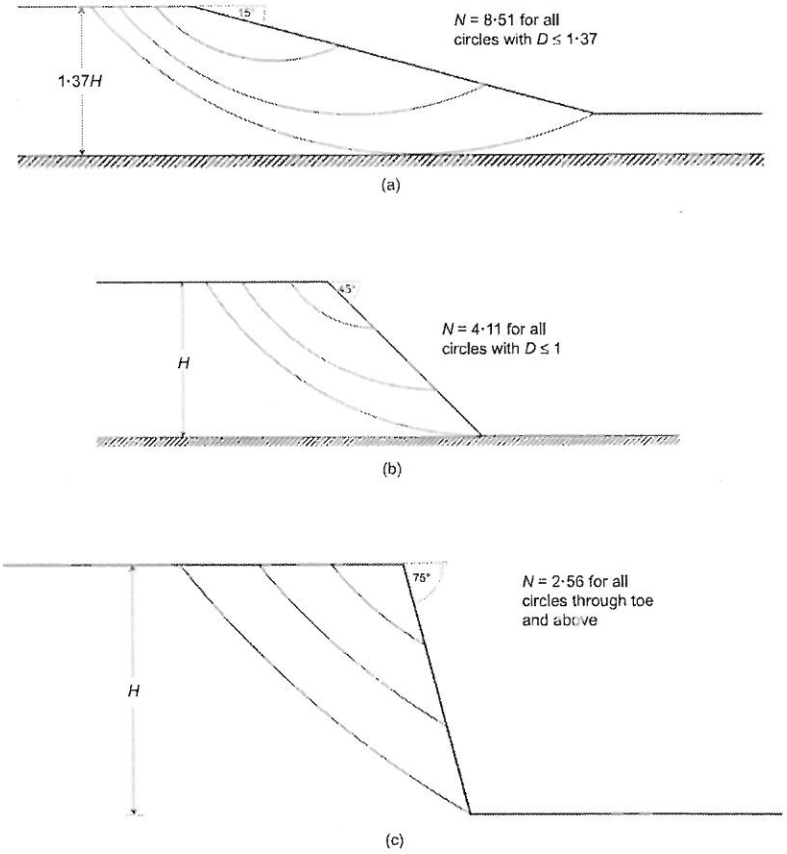

Fig. 7. Critical circles for $M=0$: (a) $\beta=15°$; (b) $\beta=45°$; (c) $\beta=75°$

Gibson and Morgenstern's comment that the critical circle giving the minimum factor of safety always lies within the slope.

CONCLUDING REMARKS

The paper has revisited the problem of an undrained slope with linearly increasing strength with depth. Results have been presented for the stability number N as a function of slope angle β, strength gradient parameter M and depth ratio D. In the case of a non-zero strength at the ground surface ($c_{u0}>0$), four critical mechanism types were identified as deep ('D'), base ('B'), toe ('T') and slope ('S'). Although the values of N computed in this paper corresponding to deep and base mechanisms (higher values of D) were in complete agreement with the published results of Hunter & Schuster (1968), the values of N computed in the toe and slope cases (lower values of D) were quite different and could be considerably higher. In the current paper, N in the toe and slope range was observed to rise steeply as $D\rightarrow 0$, in contrast to Hunter and Schuster's values, which indicated constant N with no influence of D. Complete insensitivity of N to the value of D is indeed the case when the strength at the surface is zero ($c_{u0}=0$), as noted by Gibson & Morgenstern (1962). It was observed in the current work, however, that for flatter slopes where $\beta<45°$, critical circles could extend well into the foundation and were not necessarily confined within the slope itself.

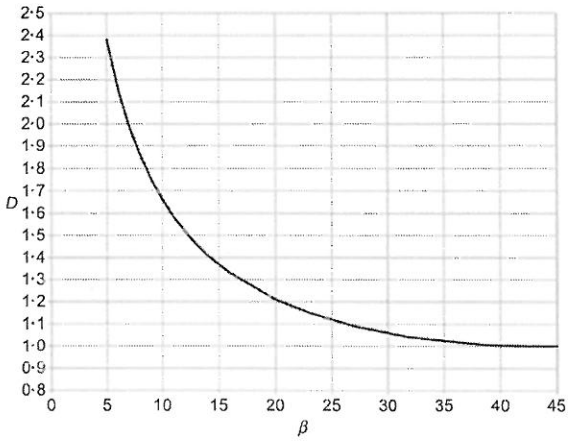

Fig. 8. Maximum depth D of critical circles for slope angle β when $M=0$

NOTATION

c_u undrained strength
c_{u0} undrained strength at crest ($z=0$)
D depth ratio
FS factor of safety
H slope height
H_0 height above crest where $c_u=0$
M strength gradient parameter
M_O overturning moment

M_R restoring moment
N stability number
z depth below crest
β slope angle
γ saturated unit weight
ρ strength gradient
ϕ_u total stress friction angle ($=0$)

REFERENCES

Booker, J. R. & Davis, E. H. (1972). A note on a plasticity solution to the stability of slopes in inhomogenous clays. *Géotechnique* **22**, No. 3, 509–513, http://dx.doi.org/10.1680/geot.1972.22.3.509.

Gibson, R. E. & Morgenstern, N. (1962). A note on the stability of cuttings in normally consolidated clay. *Géotechnique* **12**, No. 3, 212–216, http://dx.doi.org/10.1680/geot.1962.12.3.212.

Hunter, J. H. & Schuster, R. L. (1968). Stability of simple cuttings in normally consolidated clay. *Géotechnique* **18**, No. 3, 372–378, http://dx.doi.org/10.1680/geot.1968.18.3.372.

Koppula, S. D. (1984). On stability of slopes in clay with linearly increasing strength. *Can. Geotech. J.* **21**, No. 3, 577–581.

Shen, J. M. & Brand, E. W. (1985). Discussion of 'On stability of slopes in clay with linearly increasing strength' by Koppula, S. D. *Can. Geotech. J.* **22**, No. 3, 419–421.

Yu, H. S., Salgado, R., Sloan, S. W. & Kim, J. M. (1998). Limit analysis versus limit equilibrium for slope stability. *J. Geotech. Geoenviron. Engng* **124**, No. 1, 1–11.